PHYSICAL REVIEW E **66**, 015203(R) (2002)

Ratchet models using driving forces generated by deterministic chaotic maps

Cheng-Hung Chang
National Center for Theoretical Sciences, Physics Division, 101, Section 2 Kuang-Fu Road, Hsinchu 300, Taiwan
(Received 29 March 2002; published 23 July 2002)

This study investigates how ratchets perform under driving forces generated by the circle, baker, and logistic maps with varying driving frequencies. The markedly different unidirectional net transports induced by distinct maps and frequencies are clarified by vector field analysis of the ratchet equations. Analysis results indicate that both the deterministic property of the driving forces and the asymmetric effect due to the ratchet potential impact the transport. Moreover, the driving frequency determines which factor suppresses the other one and dominates the ratchet transport.

DOI: 10.1103/PhysRevE.66.015203 PACS number(s): 05.45.Ac, 05.40.Fb, 05.45.Pq, 05.60.Cd

As widely speculated, the directed net transport without external bias in a variety of physical and biological systems is ascribed to the ratchet mechanism, accounting for why diverse ratchet models have received considerable attention in the recent decade [1]. A rather general class of these models can be mathematically formulated as

$$m\ddot{x}+\gamma\dot{x}+\frac{d\,V(x,t)}{d\,x}=f(t), \tag{1}$$

which describes the motion of a particle with mass m on a periodic asymmetric potential $V(x,t)$ under a damping force with damping coefficient γ and a driving force $f(t)$ of zero mean, i.e., time average $\langle f(t)\rangle=0$. This model is characterized by its directed net transport, even when the driving force is of zero mean, i.e., the ensemble and time average $\langle x(t)\rangle \neq 0$ despite $\langle f(t)\rangle=0$ (for proper equation parameters). Studies of this model can be classified into two categories. The first category attempts to clarify how a microsystem can extract usable work from chemical or other fluctuating potentials. In this category, Eq. (1) is nothing but the Langevin equation with the Brownian particle m under a white noise damping and driven by an additional colored noise $f(t)$. A prominent biological application of this category of studies is the molecular motors [2], which are interpreted to be a plausible mechanism for muscular contraction, cell division, and intracellular transport [2]. The second category investigates how to artificially supply the external force of zero mean, e.g., $f(t)=\cos(\omega t)$, to do work such as segregating particles or rectifying currents [3]. Examples of this category can be found in diverse physical disciplines such as superconductors [4], Josephson junctions [5], quantum dots [6], geometric ratchets [7], and laser cooling [8].

In the above studies, $f(t)$ is either deterministic and predictable such as simple functions, e.g., $\cos(\omega t)$, or stochastic such as random noises, which might be induced by successive kicks correlated by some probability instead of an exact deterministic rule. However, as well known, a variety of systems in nature are governed by another class of dynamics, i.e., deterministic chaos, which can behave as stochastic as noise, while adhering to a certain deterministic property. The following question arises: How does the ratchet transport mechanism behave if the ratchet is driven by such class of forces? Notably, the previous studies [9] investigating how chaos mimicks the role of noise imply that Eq. (1) is chaotic, even when $f(t)=\cos(\omega t)$ is not a noise. That context differs from this in the current work.

To answer the above question, we study the simple ratchet model (1) driven by discrete kicks generated with deterministic chaotic maps, which include the circle map, baker map, and logistic map. The interesting transport features in which distinct maps induce diverse directions for high frequency kicks but induce the same direction for low frequency kicks imply that different factors govern the transport. A further investigation by using vector field analysis of the ratchet equation in the phase space and histogram evolution analysis in the position space reveals that the asymmetric effect due to ratchet potential and the deterministic property of the driving force are two main factors affecting the transport. Whether the asymmetric effect or the deterministic property dominates is determined by the frequency of the kicks in the driving forces. This phenomenon highlights the significant role of the deterministic property of the driving forces, which is capable of suppressing the asymmetric effect due to the ratchet potential.

Our model setup is Eq. (1), furnished with a temporally discrete driving force $f(t)$,

$$m\ddot{x}+\gamma\dot{x}+\frac{d\,V(x)}{d\,x}=\alpha\sum_{n=0}^{\infty}a_n\delta(t-\beta n), \tag{2}$$

where β denotes the period of the kicks, α represents the strength of the force, and a_n are pure numbers with zero mean, i.e., $\langle a\rangle=\lim_{\tau\to\infty}\Sigma_{n=0}^{\tau}a_n=0$. To clarify the main features of the problem, we fix the period of the kicks to keep the model simple. However, the amplitudes a_n of the kicks are deterministically chaotic in the time sequence. Without a loss of generality, we set $m=1$ and take the well-known ratchet potential, e.g., see [9],

$$V(x)=c-\frac{4\sin[2\pi(x-x_0)]+\sin[4\pi(x-x_0)]}{16\pi^2 d},$$

where $d=1.6$, $x_0=-0.190$, and $c=0.028/d$, such that the position $x=0$ is a minimum of the potential (Fig. 1). This potential has period one, and the region between two barriers at $x_-=-0.381$ and $x_+=0.619$ can be chosen as a unit cell.

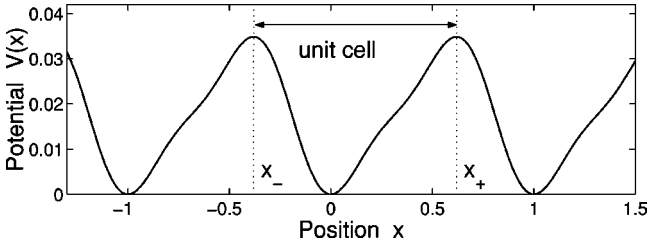

FIG. 1. Potential $V(x)$ and a unit cell between x_- and x_+.

The chaotic maps, i.e., the circle map T_C, the baker map T_B, and the logistic map T_L, are used here to drive the ratchet system. They are defined on the unit interval $I := [0,1)$ as follows:

Maps	$T : I \to I$	Invariant measure $P(z)$
Circle	$T_C : z \mapsto z + c \bmod 1$	Lebesque $P_C(z) = 1$
Baker	$T_B : z \mapsto 2z \bmod 1$	Lebesque $P_B(z) = 1$
Logistic	$T_L : z \mapsto 4z(1-z)$	$P_L(z) = \dfrac{1}{\pi\sqrt{z(1-z)}}$

The number $c = \sqrt{26}/10$ is chosen to be irrational, so that T_C is ergodic. The other two maps are not only ergodic, but also mixing and exact [10]. All these maps are deterministic and belong to different hierarchies of chaos. The last two have a positive Lyapunov exponent and their long time behavior is unpredictable. After many iterations, the distribution of the positions in the orbit $\{T^n z_0, n = 0,1, \ldots\}$ approaches an invariant probability density for almost all initial points z_0. This density can be determined analytically by the Perron-Frobenius operator $\mathcal{L}_T f(z) = \Sigma_{y \in T^{-1}z}[f(y)/|T' y|]$, where the sum extends over the preimage $T^{-1}z := \{y \in I \,|\, Ty = z\}$ [10]. The leading eigenvalue of this operator is one and the corresponding eigenfunction is the invariant density of the maps. For the above-mentioned maps, the densities are listed in the above tabular and plotted in Fig. 2. Since all these densities are symmetric with respect to the axis $z = 0.5$, the points in the orbits of the maps can be used to generate the amplitudes a_n of the deterministic driving force in Eq. (2) by the following replacement:

$$a_n = T^n z_0 - 0.5 \quad \text{for almost all } z_0 \in I.$$

Obviously, this force has a zero mean $\langle a \rangle = 0$ with $a_n \in [-0.5, 0.5)$.

A kick in Eq. (2) provides an impulse of δ form that gives a transient velocity change

$$\dot{x}(n+\epsilon) - \dot{x}(n-\epsilon) = \int_{n+\epsilon}^{n+\epsilon} f(t)\, dt = \alpha\, a_n, \quad \epsilon \ll 1,$$

while the position x remains the same directly after the kick. Between two arbitrary consecutive kicks, the particle motion is governed by Eq. (2), without the sum on the right hand side. For a large ratio γ/α, the trajectories $x(t)$ are trapped around a minimum of the potential and cannot hop over the barriers into the other unit cells. For a small ratio γ/α, the particle motion is a random walk on an asymmetric potential.

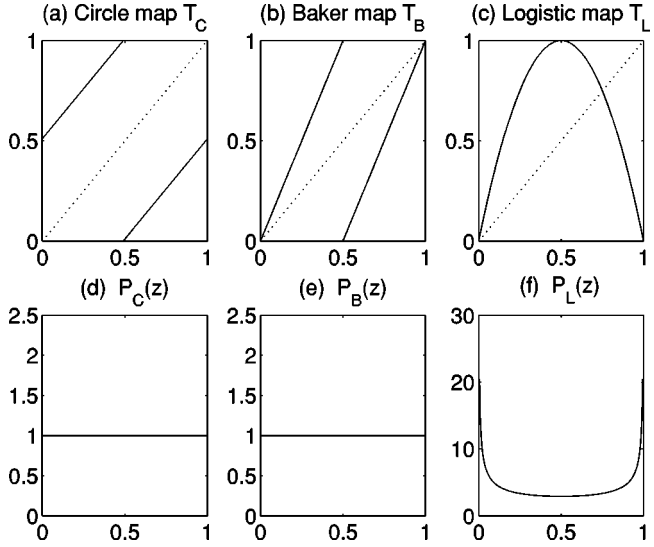

FIG. 2. (a) Circle map, (b) Baker map, (c) Logistic map, and the invariant probability densities for (d) Circle map, (e) Baker map, and (f) Logistic map.

The trajectories $x(t)$ wander between different unit cells. For a ratio γ/α between these two regions, unidirectional net transport becomes apparent, which is of interest here. To make it concrete, we take the damping coefficient $\gamma = 1$ and the period β and the strength α of the kicks as follows: (I) $\beta = 8, \alpha = 1.17$ for all maps; (II) $\beta = 1, \alpha = 0.9$ for T_C; $\alpha = 0.3$ for T_B; and $\alpha = 0.4$ for T_L. Since the long time behaviors of the trajectories are similar for different initial conditions, we show only one trajectory for every map. Their initial conditions are $(x, \dot{x}) = (0,0)$ for (I) and $(x, \dot{x}) = (-50,0)$ for (II), with $z_0 = \sqrt{11}/10$ for both cases. Interestingly, the following observations can be made (Fig. 3).

(i) For kicks with a long period, i.e., $\beta = 8$, all maps induce negative transport.

(ii) For kicks with a short period, i.e., $\beta = 1$, baker map and circle map prefer positive transport and logistic map prefers negative transport.

To clarify this peculiar behavior, we examine the phase space of Eq. (2). By using the definitions $v = \dot{x}$ and $U(x) = d\,V(x)/d\,x$, Eq. (2), without the driving term, can be rewritten as

$$\frac{d}{dt}\begin{pmatrix} x \\ v \end{pmatrix} = \begin{pmatrix} v \\ -\gamma v - U(x) \end{pmatrix}. \tag{3}$$

Above dissipative dynamics has point attractors at $(x,v) = (n,0)$ and hyperbolic fixed points at $(x,v) = (n + x_-, 0)$ for all integers n. The vector field of Eq. (3) is split into different basins, separated by stable (dashed lines) and unstable (solid lines) manifolds of the fixed points. [Fig. 4(a)]. For strong damping systems, e.g., $\gamma = 1$, the vector field structure resembles that in Fig. 4(b). For weak damping systems, e.g., $\gamma = 0.2$, the structure resembles that in Fig. 4(c). Obviously, the phase space for weak damping is more complex than that for strong damping since different basins entangle with each other.

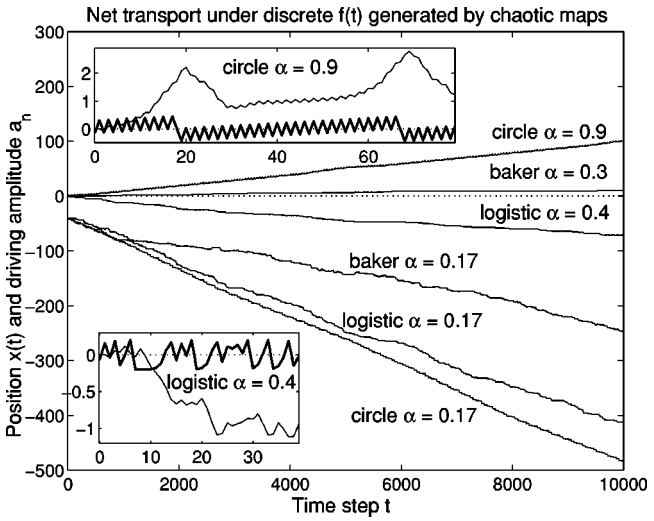

FIG. 3. Directed net transport for different maps. Three trajectories with short period $\beta=1$ begin with $x=0$. Three trajectories with long period $\beta=8$ begin with $x=-50$. For short period $\beta=1$, the first few steps of the maps T_c and T_L are magnified in the two insets, where the amplitudes $\alpha a_n, n=1,2,\ldots,$ of the driving force are connected by two thick zigzag curves.

The evolution of a state in the phase space follows the zigzag route shown in the example in Fig. 4(d). This route has two parts: a smooth one following the flow of the vector field, due to damping, and another one with many intermediate jumps in v direction, due to the kicks of the driving force. The damping force tends to drag a state in a basin toward its left boundary since the potential is asymmetric and the attractor is closer to the left boundary of its basins

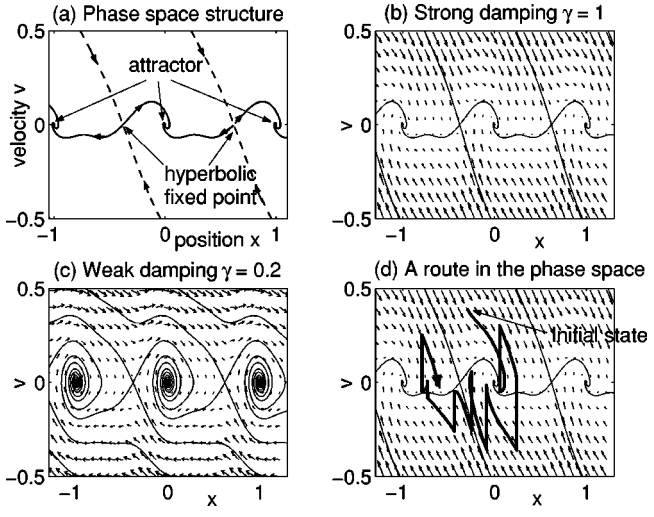

FIG. 4. The phase space of the dynamics in Eq. (3): (a) Six basins of the three attractors at (0,0) and $(\pm 1,0)$ are separated by the stable (dashed lines) and unstable (solid lines) manifolds of the two hyperbolic fixed points at $(x_-,0)$ and $(x_-+1,0)$. (b) The vector field for strong damping $\gamma=1$. (c) The vector field for weak damping $\gamma=0.2$. (d) The evolution of an initial state $(x(t),\dot{x}(t))$ governed by Eq. (2). The kicks provide vertical jumps and the dynamics between kicks follows the vector field of Eq. (3).

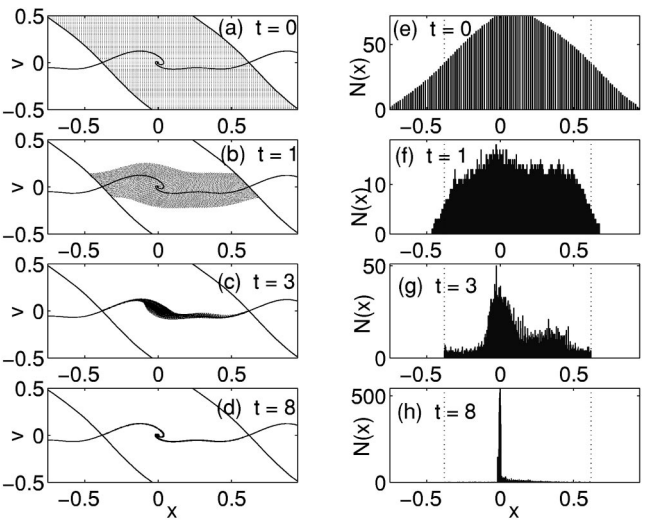

FIG. 5. Evolution of an ensemble of initial states in the phase space and the corresponding evolution of positions in the configuration space. (a), (b), (c), and (d) are the distributions of states in the phase space at time $t=0$, 1, 3, and 8. (e), (f), (g), and (h) are the corresponding position histograms.

than the right one. Thereafter, a random kick has a higher likelihood of pushing the state over the left boundary than the right boundary, assuming that the time span between two kicks is not too short. This effect is significant when the damping γ is strong. Of course, α must be enhanced simultaneously to maintain the ratio γ/α. The closer the attractor is to the left boundary (i.e., the steeper is the left wall of the unit cell) creates a strong asymmetric effect. For a weak damping system, the basins of different attractors entangle with each other. A state spirals for a long time before arriving at the attractor. The next kick has a higher likelihood of coming before the state has been trapped close enough to the attractor. In this case, the directed net transport can no longer be as easily observed as a system with strong damping. In conclusion, due to the asymmetric effect, the system prefers to induce a negative current independent of whether the kicks are random or deterministic. This current is apparent, as long as the kick period β is large.

For a short kick period β, the asymmetric effect is slight. It can be realized by observing the evolution an ensemble of 4969 uniformly distributed states (x,v) in the basins of the attractor (0,0) bounded by $|v|<0.5$ [Fig. 5(a)]. Therein, 50.51% of these states are located on the left hand side of the center $x_c=(x_++x_-)/2$ of the unit cell. Owing to the dissipative nature of the system, all states are contracted into the attractor. However, the contraction is mainly along the direction of the stable manifolds for most initial states. Only those states with a small $|v|$ obtain a stronger contraction parallel to the x direction toward the attractor, as indicated in the ensemble evolution shown in Figs. 5(a), 5(b), 5(c), and 5(d) for $t=0$, 1, 3, and 8. The corresponding histograms of the position distribution are shown in Figs. 5(e), 5(f), 5(g), and 5(h), with 50.51%, 52.59%, 61.58%, and 89.92% of the states on the left hand side of x_c. For a system with a short period, e.g., around $\beta=1$, a state obtains successive kicks before becoming trapped into the attractor. In this case, the

transport into left and right basins, induced by kicks, is nearly equal. For such β regime, the asymmetric effect contributes only weakly to the directed transport. Therefore, the deterministic property of the driving force induced by different chaotic maps becomes apparent for the transport direction.

Next, an attempt is made to understand why the deterministic property of the driving force significantly affects the transport direction for small β by closely examining the trajectory $x(t)$ in the insets of Fig. 3. The magnitudes αa_n of the impulses supplied by the kicks are connected by the thick curves. According to the insets, the particle can climb over the right boundary when the system can accumulate a large net force $|\alpha \Sigma_{\tau_1}^{\tau_2} a_n|$ within a short time span between some τ_1 and τ_2. An apparent example can be found in the circle map for $\tau_1 = 20$ and $\tau_2 = 66$ in the upper inset of Fig. 3. This deterministic property generated by the circle map overcomes the asymmetric effect and leads to a positive transport. Conversely, this force accumulation effect for the logistic map is weak, (bottom inset in Fig. 3), accounting for why the transport direction induced by this map remains negative.

In summary, this work has attempted to understand the transport behavior of ratchet models under a different class of driving forces, i.e., deterministic chaos, and in doing so, studies ratchet models driven by the circle map, baker map, and logistic map. The diverse transport directions induced by distinct maps imply the significance of the deterministic property of the forces. This property can overcome the asymmetric effect due to the ratchet potential for a high frequency driving force and dominates the ratchet transport. This work provides further insight into the ratchet transport mechanism, especially with respective to how deterministic chaos affects the ratchet transport.

The author would like to thank the National Science Council of the Republic of China, Taiwan, for financially supporting this research under Contract No. NSC 90-2112-M-007-067. T.Y. Tsong, W. Wang, and J. Wang are appreciated for their encouragement and valuable discussions.

[1] P. Reimann, Phys. Rep. **361**, 57 (2002); R.D. Astumian, Science **276**, 917 (1997); F. Jüdlicher, A. Ajdari, and J. Prost, Rev. Mod. Phys. **69**, 1269 (1997).

[2] T.Y. Tsong and T.D. Xie, Appl. Phys. A, http://dx.doi.org/10.007/S003390101057; T.Y. Tsong and R.D. Astumian, Bioelectrochem. Bioenerg. **15**, 457 (1986); T.D. Xie, P. Marszalek, Y.d. Chen, and T.Y. Tsong, Biophys. J. **67**, 1247 (1994); T.D. Xie, Y.d. Chen, P. Marszalek, and T.Y. Tsong, *ibid.* **72**, 2496 (1997); M.O. Magnasco, Phys. Rev. Lett. **71**, 1477 (1993); R.D. Vale and F. Oosawa, Adv. Biophys. **26**, 97 (1990); S.C. Kuo and M.P. Sheetz, Science **260**, 232 (1993); G. Lattanzi and A. Maritan, Phys. Rev. Lett. **86**, 1134 (2001); B. Alberts, D. Bray, J. Lewis, M. Raff, K. Roberts, and J.D. Watson, *Molecular Biology of the Cell* (Garland, New York, 1994).

[3] J. Rousselet, L. Salome, A. Ajdari, and J. Prost, Nature (London) **370**, 446 (1994); P. Hänggi and R. Bartussek, in *Nonlinear Physics of Complex Systems*, edited by J. Parisi, S.C. Müller, and W. Zimmermann, Lecture Notes in Physics Vol. 476 (Springer-Verlag, Berlin, 1996), pp. 294-308. The works of Tsong *et al.* in Ref. [2].

[4] C.-S. Lee, B. Jankó, I. Derényi, and A.-L. Barabási, Nature (London) **400**, 337 (1999).

[5] I. Zapata, R. Bartussek, F. Sols, and P. Hänggi, Phys. Rev. Lett. **77**, 2292 (1996); E. Goldobin, A. Sterck, and D. Koelle, Phys. Rev. E **63**, 031111 (2001).

[6] H. Linke, W. Sheng, A. Löfgren, H. Xu, P. Omling, and P.E. Lindelof, Europhys. Lett. **44**, 341 (1998).

[7] M. Bier, M. Kostur, I. Derényi, and R.D. Astumian, Phys. Rev. E **61**, 7184 (2000); A. van Oudenaarden and S.G. Boxer, Science **285**, 1046 (1999).

[8] C. Mennerat-Robilliard, D. Lucas, S. Guibal, J. Tabosa, C. Jurczak, J.-Y. Courtois, and G. Grynberg, Phys. Rev. Lett. **82**, 851 (1999).

[9] J.L. Mateos, Phys. Rev. Lett. **84**, 258 (2000); P. Jung, J.G. Kissner, and P. Hänggi, **76**, 3436 (1996).

[10] A. Lasota and M.C. Mackey, *Chaos, Fractals, and Noise* (Springer-Verlag, Berlin, 1994).